Nuclear Instruments and Methods in Physics Research A 652 (2011) 591–594

Contents lists available at ScienceDirect

Nuclear Instruments and Methods in Physics Research A

journal homepage: www.elsevier.com/locate/nima

# Spatial calibration via imaging techniques of a novel scanning system for the pulse shape characterisation of position sensitive HPGe detectors

N. Goel *, C. Domingo-Pardo, T. Engert, J. Gerl, I. Kojouharov, H. Schaffner

*GSI Helmholtzzentrum fuer Schwerionenforschung GmbH, Planckstr. 1, 64291 Darmstadt, Germany*

ARTICLE INFO

Available online 4 February 2011

*Keywords:*
PSD
Gamma camera
PSC
Germanium

ABSTRACT

In this work, a novel imaging technique for the spatial calibration of a gamma camera is presented. The latter is aimed for the characterisation of the charge signals of 3D-position sensitive HPGe detectors. The characterisation method itself is based on pulse shape comparison (PSC) technique. The performance of the device is improved by implementing a gamma camera or position sensitive detector (PSD). This PSD consists of a uniform LYSO scintillating crystal optically glued to a crossed-wire position sensitive photomultiplier tube (PSPMT) from Hamamatsu. The individual multianode readout (IMAR) approach is used to improve its spatial resolution and to enlarge its field of view. A Compton scattering imaging technique is implemented to perform an accurate position calibration of the gamma camera.



## 1. Introduction

The core principle of segmented germanium detector arrays like AGATA [1], GRETA [2], that will be used in future for $4\pi$ gamma detection arrays, is the application of the concept of pulse shape analysis (PSA) and gamma ray tracking [3]. For $\gamma$-ray tracking algorithms, it is required to measure the position coordinates and the energy deposited for each $\gamma$-ray interaction point inside the detector. The scattering path of the photon inside the detector can then be reconstructed using the Compton scattering formula. The precision of a $\gamma$-ray tracking algorithms is strongly dependent on how accurately the interaction positions are determined. The 3D-position sensitivity of the HPGe detectors is based on the difference in the shape of the charge pulses associated with different interaction points inside the whole volume. The aim of pulse shape analysis is to create a database containing pulse shapes for all the interaction points inside the detector volume. A full 3D scanning of the detector, which experimentally determines pulse shapes for every given position inside the active volume, is therefore needed. There are conventional 3D scanning systems available [6], which are based on collimated sources for selecting a $\gamma$-ray direction. The interaction depth is determined by demanding 90° Compton scattering into appropriate gamma detectors located around the germanium detector to be scanned. Even with strong sources the scanning process with such a system takes several months for large volume germanium detectors. We developed a novel system aiming at determining pulse shape database for HPGe detectors within only few days. The performance and efficiency of the system strongly depends on a position sensitive detector (PSD). This paper reports on the characterisation tests performed for the PSD namely its position calibration using Compton scattering imaging techniques for its successful application in the aforementioned scanning system.

## 2. Principle of the scanner

We proposed and implemented a first detector scanner based on the principles of pulse shape comparison (PSC) [4] and positron annihilation correlation (PAC) [5]. A 300 KBq point like $^{22}$Na positron source emitting two 511 keV photons in opposite directions is placed between the position sensitive detector (PSD) and the germanium detector to be scanned (Fig. 1). The trajectories of $\gamma$-rays entering the germanium volume are determined by the PSD. This allows creating a "collimation-free" scanner, where many lines across the detector or even the whole detector can be scanned simultaneously in each projection. For the position (a) in Fig. 1, a database containing pulse shapes for all the trajectories coming inside the coincidence cone of the Ge and the PSD is recorded. The $(x,y)$ coordinates measured in the PSD provide the trajectories of $\gamma$-rays. For a second measurement, corresponding to the position (b) in Fig. 1, the PSD and $^{22}$Na are rotated together around the Ge detector. In Fig. 1, it is shown that they are rotated by 90°. Again a data set containing the pulse shapes and the $(x,y)$ coordinates given by the PSD for this

* Corresponding author.
*E-mail address:* n.goel@gsi.de (N. Goel).

0168-9002/$ - see front matter © 2011 Elsevier B.V. All rights reserved.
doi:10.1016/j.nima.2011.01.146

configuration is recorded. If these two data sets are compared, the only case where a signal of one set is identical to the signal of the other set is when the two signals correspond to the crossing point of two lines inside the coincidence cone. In this way, it is possible to obtain a database containing the pulse shape for each crossing point. The (*x*,*y*,*z*) coordinates of the crossing point are determined from the two $\gamma$-ray trajectories measured via the PSD. The main feature of the PSCS is that it allows to obtain the pulse shape database for a HPGe detector much faster as compared to the conventional scanning methods [6]. The pulses for a particular interaction point are selected on the basis of a $\chi^2$ comparison test, similar to the method described in Ref. [4]. The experimental results obtained for a nonsegmented planar germanium detector will be discussed in a forthcoming paper. The position resolution achieved in the scanning system depends on the spatial resolution of the PSD. The PSD is described in detail in Ref. [8] and for the sake of completeness its main features are summarized in Section 3. Section 4 explains the position calibration of the detection system using the Compton scattering imaging techniques.

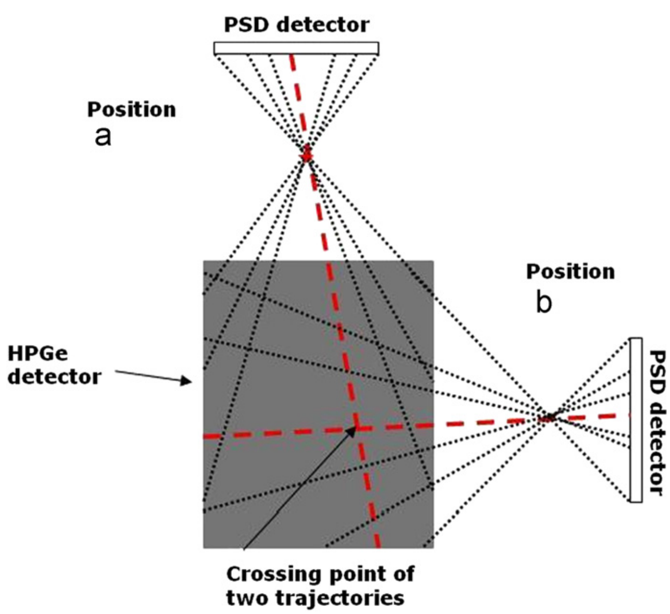


**Fig. 1.** Pulse shape comparison scan of germanium: (a) pulse shapes recorded for the collimation lines coming inside the coincidence cone of PSD and germanium and (b) source and PSD moved together by an angle of 90° and again a data set of pulse shapes is measured.

## 3. Gamma camera

State-of-the-art small position sensitive $\gamma$-ray detectors (PSDs) are normally made from a relatively thin scintillation crystal, which is optically coupled to a position sensitive photomultiplier tube (PSPMT). A frequently used PSPMT is based on a crossed-wire anode structure, e.g. the Hamamatsu R2486/3292 family. The anode of the R2486 consists of two orthogonal layers of 16 wires in the *X*-axis and 16 in the *Y*-axis, on a pitch of 3.75 mm. In order to simplify the readout process, the wires within each layer are often connected to a resistive charge dividing network such that only four outputs are required to determine the centroid of the electron cloud reaching the anode. However, we showed that a substantial improvement in the intrinsic spatial resolution, position linearity and in the useful field of view (FoV) of the detector can be achieved by individual multianode readout (IMAR) as compared to the resistive network (RN) approach as it is reported in Ref. [8]. Our detector system consists of a cylindrical LYSO crystal with 76 mm diameter and 3 mm thickness, optically coupled to a Hamamatsu R2486 PSPMT. Using the IMAR method, it is possible to calibrate the gain of individual anodes. From the calibrated charge distributions measured along *X* and *Y* anodes, the interaction position (*x*,*y*) is determined via several algorithms and two of them are shown in Fig. 2. The surface of photocathode is scanned using a collimated $^{22}Na$ source. The panel (a) in Fig. 2 shows the performance of the Gauss-fitting approach. The peak position of the Gaussian fit for both *X* and *Y* anodes gives the position (*x*,*y*). This approach works relatively well in the central region of the photocathode, where the charge distributions are still rather symmetric. However, towards the border of the photocathode two additional effects take place. The scintillation charge profile is near the edge of the photocathode and we measure only a part of it. The peak position of the Gaussian fit for the truncated charge distribution will deviate from the real position. Also the light reflections at the edge region of the scintillation crystal affect the measured charge profile. These two effects result in non-linearity in the position distribution near the edges of the PMT which is evident in panel (a) of Fig. 2. The second algorithm is based on a pattern fitting approach. An average charge profile is created from the average of large number of charge distributions at the centre of the photocathode. This average charge profile is then fitted using a realistic scintillation light distribution model reported by Lerche [7] and stored in a fine binned (0.05 mm) numerical pattern. When charge distribution is measured for any other location on the photocathode surface, it is compared with the stored numerical pattern. The relative position of the pattern is varied until it matches with the measured charge distribution using a $\chi^2$

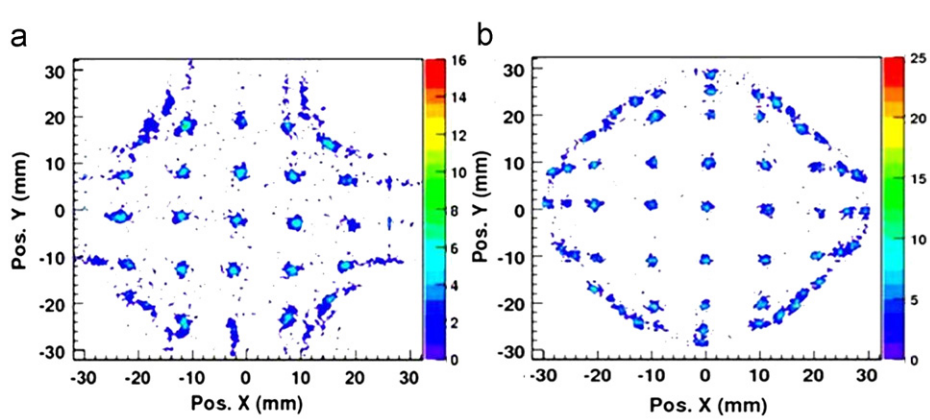


**Fig. 2.** (a) Gaussian fitting approach. (b) Pattern-position fitting approach.

minimisation. The panel (b) of Fig. 2 illustrates the improvement obtained in the determination of the (*x,y*) coordinates, when the pattern fitting approach is implemented. The system is remarkably linear with an enhanced FoV using the IMAR method. It is linear 50 mm along the photocathode, in both *X* and *Y* directions. The FoV with the IMAR technique is about 19 cm$^2$ assuming a circular FoV.

On average, along the *X*- and *Y*-axes of the PSPMT, we have measured position distributions with an equivalent FWHM of better than 1 mm for positions along the *X*- and *Y*-axes (see Ref. [8] for details). The average intrinsic efficiency of the PSD for 511 keV $\gamma$-rays is experimentally determined as $\varepsilon_{\gamma}^{FE} = 7.5 \pm 1.5\%$ for full energy events. These qualities make this system suitable for our aim and very attractive for many $\gamma$-ray imaging applications.

## 4. Position calibration using Compton scattering imaging techniques

After the characterisation of the position sensitive detector, it is placed in the scanning system. The $^{22}$Na source is at a fixed distance of $(5.5 \pm 0.5)$ cm from the surface of the PSD. The central axis of the scanning system is at a distance of $(15 \pm 1)$ cm from the source. The centre of gravity of the germanium detector which is to be scanned is placed in the vicinity of the rotation axis of the scanner. The image size of the detector to be scanned depends on its distance to the source and varies with the interaction depth due to the 3D spatial occupancy of the detector volume. In order to get an image as close as possible to the real object, a position calibration of the gamma camera is needed.

To implement the position calibration, a $(11 \times 11)$ cm$^2$ steel grid with 2 mm thick grid lines separated by 1 cm is placed in front of the source and PSD detector assembly. It is made sure that the central axis of the grid coincides with the central axis of the scanning table. This grid is the reference object and the aim now is to get an image of it in the PSD which allows us to determine the correspondence between the real ($x_r$, $y_r$) and measured ($x_m$, $y_m$) positions of the grid crossing lines. To get the image of the steel grid, a $\gamma$-ray scattering technique [9] is implemented. For 511 keV $\gamma$-rays from $^{22}$Na source, the dominant mode of interaction in steel is Compton scattering. For an event, two 511 keV photons are emitted by the $^{22}$Na source in opposite directions. One of them impinges the PSD and the other photon gets Compton scattered off the grid and is registered in one of the two NaI(Tl) scintillators placed at forward angles (Fig. 3). The acquisition system is triggered to register the coincident events between the position sensitive detector and the NaI detectors. For a particular event only one of the NaI is activated depending on the direction where photon gets scattered off the grid. An image has been reconstructed using the coincidence events for this setup and applying the pattern fitting algorithm (Fig. 4(a)). The black square around the grid image gives an estimate of its measured size. The projected image on PSD is inverted and the events on the top of the position matrix show the presence of the support holding the grid. For each real position coordinate ($x_r$, $y_r$) there corresponds a measured position coordinate ($x_m$, $y_m$) on the image of the grid. For example, the measured position coordinates of the point marked in Fig. 4(a) are (4.31, 4.30) mm, which in real space correspond to (10,10) mm.

The exact functional relationship between the measured points and the real points is not known, but it depends on the linearity of the system and also on the source-PSD distance. One possible way of solving the problem is to find an expression which reliably approximates the dependence of the real position coordinates on the measured ones. The positions given by the crossing points of two orthogonal grid lines are used for the position calibration. For each measured position on the grid, the corresponding real coordinate is known. We used a position reconstruction method [10,11] based on a 2D polynomial functional fit to the measured data. For a finite number of measured points on the grid, the behaviour of the system can be described by two functions *f* and *g*.

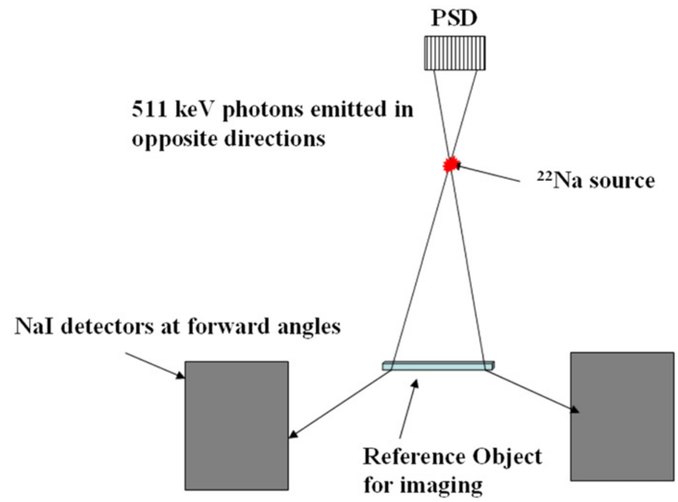


**Fig. 3.** Principle of Compton scattering imaging technique.

$$f(x_m,y_m) = \sum_{j=1}^{M} C_j x_m^{a_j} y_m^{b_j}, \quad g(x_m,y_m) = \sum_{j=1}^{N} D_j x_m^{c_j} y_m^{d_j} \tag{1}$$

where $C_j$, $D_j$, $a_j$, $b_j$, $c_j$ and $d_j$ are the coefficients. To fit the data, CERN ROOT class TMultiDimFit [12] is used. Fig. 4(b) plots the reconstructed positions (red circles), to be compared with the real positions (solid squares), when the fitted analytical functions *f* and *g* are applied to all the measured points (green triangles).

The position calibration method explained above is first applied to the case when the steel grid is parallel to the surface of the PSD. The calibration done for this configuration is equivalent of doing a calibration for points along any plane as shown in panel (a), Fig. 5 inside the germanium detector. This position of the grid provides about 100 points for the calibration. As the volume of germanium can be represented by these planes, it is required to extend the calibration procedure to the points along some other planes too. The grid is thus rotated in steps of 10° for four angles and the same measurement (as demonstrated above) is done for each angular position of the grid. When the grid is rotated by an angle $\theta$, the position coordinates ($x'_r$, $y'_r$) in the rotated frame are given by the following equations:

$$x'_r = \frac{D_{SG} x_r \cos\theta}{D_{SG} - x_r \sin\theta}, \quad y'_r = \frac{D_{SG} y_r}{D_{SG} - x_r \sin\theta} \tag{2}$$

where $D_{SG}$ is the distance between the source and the grid, which in our case is 150 mm and ($x_r$, $y_r$) are the position coordinates before rotation. Fig. 5(b) shows an image of the matrix when it is rotated by 40°. The 2D functions *f*' and *g*' gave good agreement between the reconstructed and real positions (calculated using Eqs. (1) and (2)) for this set of measurement positions. The maximum deviation (in mm) of the reconstructed positions from the real positions in *X* and *Y* directions are 1.178 and 1.026, respectively. The corresponding values for mean deviation in *X* and *Y* directions are 0.376 and 0.591 mm, respectively. Using the positions from all the data sets corresponding to measurements at 0°, 10°, 20°, 40°, a global 2D reconstruction function is evaluated using approximately 350 points for the calibration. This function is able to reconstruct the positions with a maximum deviation of 3.7 mm in *X* and 2.7 mm in *Y* directions. This concluded the

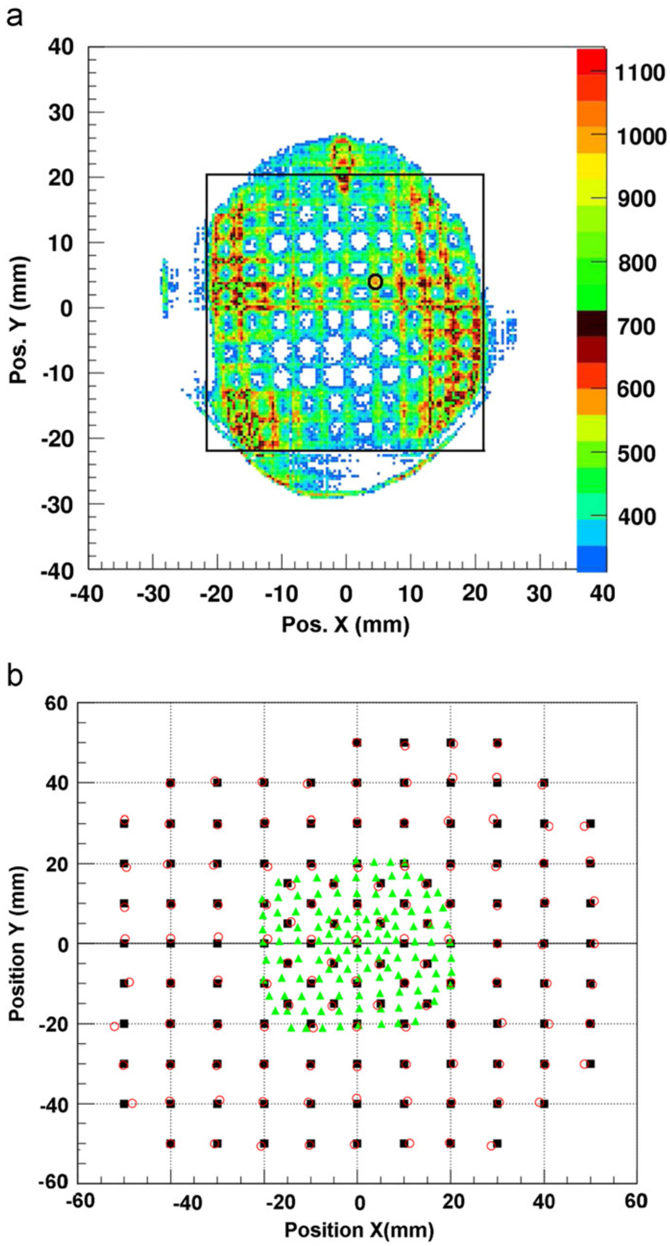


**Fig. 4.** (a) Image of the grid obtained with the position sensitive detector using the pattern fit algorithm. (b) Reconstruction of measured positions by applying 2D functions. The green triangles are the measured positions, black squares are the real positions and the red circles are the corresponding reconstructed points. (For interpretation of the references to color in this figure legend, the reader is referred to the web version of this article.)

position calibration of the gamma camera for a case when it will shine the germanium detector from the front side. According to the principle of operation of the scanning system, the source and the PSD assembly will be moved by 90° to shine the detector sideways. In principle, the same position calibration should be applicable to this configuration of the system. To check this, the same position calibration procedure is repeated for the data points measured for the 90° rotated position of the PSD. The reconstruction function found for this case is different for the one found for the 0° position of the PSD. This can be explained by the change in the mechanical alignment of the PSD when it is rotated by 90°. When the global reconstruction function obtained for 90° position is applied to the measured data set of 0° position, we get

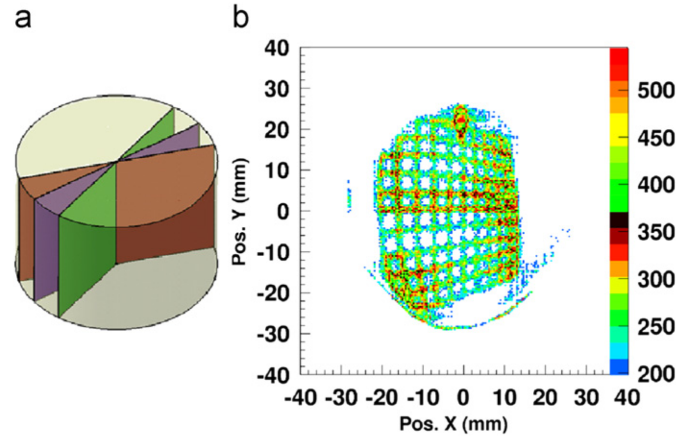


**Fig. 5.** (a) Multiple planes inside the detector volume. (b) Image of the grid when it is rotated by 40°, obtained with the position sensitive detector using the pattern fit algorithm.

a maximum deviation of 5.9 mm in $X$ and 2.9 mm in $Y$, which is greater than the deviations obtained before. So to correct for this inhomogeneity, separate reconstruction functions are obtained for different positions of the PSD at the scanning table. It is foreseen that this difficulty will be overcomed by improving mechanical aspects of the present scanning table.

## 5. Conclusions

In this work, an imaging method to perform an accurate spatial calibration of a position sensitive detector(PSD) is presented. The characterisation tests carried out on the PSD showed a spatial resolution of 1 mm (FWHM) and a very large field of view of 19 $cm^2$ and the details are reported in Ref. [8]. The calibration of later is carried out by using a Compton scattering imaging technique. The scattering of photons from a steel grid to the surrounding NaI(Tl) scintillator detectors provided the positions for calibration. A 2D polynomial functional fit is implemented to transform the measured positions to the real positions of the grid crossing lines. Mean deviations of less than 0.6 mm in $X$ and $Y$ directions are achieved with this accurate calibration procedure. The gamma camera after its successful position calibration is ready to be implemented in the scanning system meant for the position characterisation of 3D-position sensitive HPGe detectors.

## References

[1] J. Gerl, W. Korten, AGATA Technical Proposal, 2001.
[2] I.Y. Lee, et al., Nuclear Physics A 520 (November) (2004) 255.
[3] D. Bazzaco, Nuclear Physics A 746 (2004) 248c.
[4] F.C.L. Crespi, et al., Nuclear Instruments and Methods in Physics Research A 593 (August) (2008) 440.
[5] J. Gerl, et al., Nuclear Instruments and Methods in Physics Research A 525 (2004) 328.
[6] M. Descovich, et al., Nuclear Instruments and Methods in Physics Research A 553 (2005) 512.
[7] C.W. Lerche, et al., Nuclear Instruments and Methods A 537 (January) (2005) 326.
[8] C. Domingo-Pardo, et al., IEEE Transactions on Medical Imaging 28 (December) .
[9] J. Gerl, Nuclear Instruments and Methods in Physics Research A 752 (2005) 688c.
[10] B. Escat Paricio, Ph.D. Thesis, University of Valencia, 2003.
[11] M.M. Fernandez, et al., Nuclear Instruments and Methods in Physics Research A 527 (2004) 92.
[12] R. Brun, F. Rademakers, Nuclear Instruments and Methods in Physics Research A 389 (February) (1997) 21.